Fractal feature analysis of the human brain structures in neuroanatomy changes

Olena Buczko[*], Paweł Mikołajczak

*Faculty of Mathematics, Physics and Computer Science, University of Maria Curie-Skłodowska,
Pl. M.Curie-Skłodowskiej 1, 20-031 Lublin, Poland*

Abstract

The paper presents a method to examine brain structures in neuroanatomy changes which result in dementia in magnetic resonance images by using fractal analysis techniques. We measured the relationship between the fractal dimensions of white matter and grey brain matter and the relationship between the fractal dimensions of the forebrain and the white brain matter. The investigation showed that the relationship between the fractal dimensions of brain in neuroanatomy changes differ from that in the normal brain.

1. Introduction

There are a lot of diseases with a collection of symptoms described by the term dementia a number of disorders which contribute to neuroanatomy changes in the brain. Patients with dementia have significantly impaired intellectual functioning which interferes with normal activities and relationships. Some of the diseases that result in the symptoms of dementia are Alzheimer's disease, vascular dementia, Huntington's disease, Parkinson's disease, Creutzfeldt-Jakob disease [1].

Medical imaging modalities have been developed for acquisition of high-resolution images: the computed tomography (CT), the magnetic resonance (MR) imaging allowing the study by clinicians and experts a lot of body parts and detecting structural abnormalities, have shown a complex structural brain changes in dementia such as white matter volume decreases while grey matter increases. The grey matter known as the cerebral cortex is the outer layer of the brain; it covers the nuclei deep within the cerebral hemisphere known as the white matter [2].

The purpose of this study was to examine normal brain and brain in neuroanatomy changes in MR images using the fractal feature analysis and to

---

[*]Corresponding author: *E-mail address*: obuchko@gmail.com

distinguish between normal and abnormal states. MR imaging provides images with excellent contrast detail between different tissues with very similar densities, for instance gray and white matter in the brain.

Fractal analysis techniques have recently attracted much interest in image processing reported by many examples of applying to study a wide range of objects in biology and medicine, for example to detect micro-calcification in mammograms [3], small peripheral lung tumors [4], to diagnose blood cells [5], to predict osseous changes in ankle fractures [6], to analyze bone [7]. Fractal analysis allows examining structural changes of biological and medical objects because the fractal dimension value reflects alterations of structural properties.

2. Fractal dimension

Fractal is an irregular geometric object with an infinite nesting of structure of different sizes. The most important properties of fractals are self-similarity, chaos and non-integer fractal dimension. Fractals are self-similar, which means that copies can be found on different scales of size. The fractal dimension is the main characteristic of fractals. The fractal dimension is often considered as a parameter describing morphological complexity of objects and can be introduced in different ways.

Mandelbrot [8] used the term "topological dimension" to describe shapes of Euclidean objects which exist in integer dimensions, single dimensional points, one-dimensional lines and curves, two-dimensional plane figures like circles and squares, and three-dimensional solid objects such as spheres and cubes. However, many complex objects in nature are described better with fractal dimension which is a non-integer value that lies strictly in the Euclidean space, being part of the way between the two whole numbers. While a straight line has a dimension of exactly one, a fractal curve will have a dimension between a straight line and a plane (between one and two), depending on how much space it takes up as it curves and twists. A fractal surface will have dimension between a plane and three-dimension space (between two and three). A fractal object possesses the fractal dimension strictly greater than its topographical dimension.

Several definitions of fractal dimension have been proposed, such as Hausdorff-Besicovitch dimension, Bouligand-Minkowski dimension, Tricot dimension, and others [9]. In practice, Mandelbrot [8] has popularized the Hausdorff-Besicovitch dimension or mass dimension (as the measure is very often a mass), which turns out to be one of the simpler and more understandable dimensions. The equation for the Hausdorff-Besicovitch dimension, D_H is defined as:

$$D_H = \lim_{r \to 0^+} \frac{\ln N}{\ln(1/r)},$$

where *N* is the number of self-similar pieces, with the magnification factor, *1/r*, into which a figure may be broken.

3. Segmentation of white matter and grey matter

The techniques that are used to find the regions of interest are known as segmentation. Segmentation plays an important role for identification of anatomical structures and analyzing neuroanatomy changes in brain structures. The good quality of "extracting" useful information from the image, measurement accuracy strongly depends on the quality of the applied segmentation procedures.

A great number of segmentation techniques have been proposed, excellent reviews of established techniques for image segmentation were done by Pal and Pal [10], Zhang and al [11]. But it is impossible to choose one dominating technique in medical image processing that can produce good results for different anatomical objects. What kind of segmentation technique to use or different techniques together depends on the type of image data, analyzing anatomical object and the goal of the investigation.

For segmentation of white brain matter and grey brain matter we used thresholding, the region growing algorithm together with morphological operations. We segmented first the forebrain and then the white brain matter. The forebrain is the largest part of the brain (white matter and gray brain matter together) (Fig. 1.b, 1.e), which is made up of the cerebrum [2]. As a result, we have three regions: white region – white brain matter, grey region – grey brain matter, black background (Fig. 1.c, 1.f).

In the first step we segmented the forebrain by thresholding. Thresholding is the simplest and commonly used method of segmentation. A parameter T is the threshold and applied to the image *a[nr,nc]* as follows:

$$a[nr,nc] = \begin{cases} w, & if \ \ a[nr,nc] > T, \\ b, & if \ \ a[nr,nc] \le T. \end{cases} \tag{1}$$

where pixels are classified as *w* – the white regions of interest or *b* – the dark background.

We used iterative technique for choosing a threshold [12] that based on algorithm that sequentially refines an initial estimate of a suitable threshold level. The histogram is initially segmented into two parts using a starting threshold value $T_{t,0}$ such as the mean gray level for all pixels. On each iteration, the mean gray level for all pixels below the threshold $T_{t,k}$ is determined, and is denoted as $T_{w,k}$. The mean gray level for all pixels greater or equal to the threshold level $T_{t,k}$ is also determined, and is denoted as $T_{b,k}$. The new threshold $T_{t,k+1}$ is estimated until the threshold value does not change any more. In the formula:

$$T_{t,k+1} = \frac{\left(T_{w,k} + T_{b,k}\right)}{2} \quad \text{until} \quad T_{t,k+1} = T_{t,k} . \tag{2}$$

A general equation for estimating the threshold $T_{(t,k+1)}$ using the image histogram *hist* is:

$$T_{t,\,k+1} = \frac{\sum\limits_{i=0}^{T_{t,k}} i \cdot hist[i]}{2\sum\limits_{i=0}^{T_{t,k}} hist[i]} + \frac{\sum\limits_{j=T_{t,k}+1}^{N} j \cdot hist[j]}{2\sum\limits_{j=T_{t,k}+1}^{N} hist[j]}, \tag{3}$$

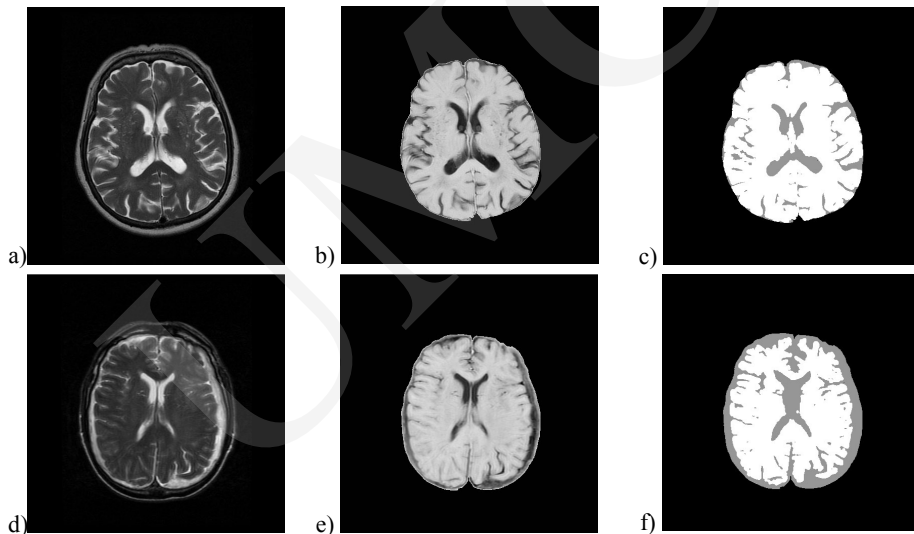*N* is the total number of pixels in the image.

Fig. 1. (a, d) the original brain MR image, (b, e) segmented image of forebrain (and inverted original pixels that lie in that region), (c, f) segmented image of white brain matter and gray brain matter

In the second step after the thresholding operation for isolation the segmented region of interest, forebrain (white matter and gray brain matter), we used the procedures:
- morphological open,
- labeling for white regions of interest,
- relabeling for white regions of interest,
- labeling for dark background.

Morphological operations based on geometrical relationship or connectivity of pixels. The combination of erosion followed by dilation is called opening [13]. The opening operation tends to smooth contours in an image, breaks narrow sections and eliminates thin protrusions. In the procedure labeling all

regions of pixels with the same intensity being found in the image and each of them being labeled, the connectivity style, uses the seeded region growing method. The seeded region growing method is based on eight neighborhood connectivities. In the procedure relabeling regions sort according to size and keep only the largest: the region of interest. Finally we used the arithmetic operation invert for original pixels that lie in our region of the forebrain.

For segmentation of the white brain matter the same operations are used as for segmentation of the forebrain but in thresholding operation the threshold is fixed and the procedure labeling dark background is employed.

4. Fractal dimension estimation

For estimation of fractal dimension of white brain matter and grey brain matter we used the methods:
– box counting,
– hand and dividers.

The box counting method is one of the wide variety algorithms for estimating the fractal dimension of a fractal object [14]. It works by covering image with boxes and then evaluating how many boxes N are needed to cover fractal completely. Repeating this measurement with different sizes of boxes r will result into the logarithmical function of the box size $(\log(1/r))$ and the number of boxes needed to cover the fractal $(\log N)$. The fractal dimension D of the object can be estimated from a linear regression defined by $\log(N(r)) = D \cdot \log(1/r) + const$.

The hand and dividers method (also called "structured walk technique" or "yardstick method") is the oldest method based on perimeter estimation using "step" or "yardstick" of different sizes [8]. This dependence can be mathematically expressed as the relation $P(X) \propto \lambda^a$, where $P(X)$ is the perimeter of the object X, λ is the yardstick size and a is the slope of the line observed in the $\log(P(X))$ vs. $\log(\lambda)$ plot. This slope is connected to the fractal dimension D as $D = 1 - a$.

The hand and dividers method can be established in the following way. At first the contour of an object is obtained using a crack following method [15], resulting in a set of contour points $\{(x_i, y_i)\}$ (Fig. 2). Then for a given yardstick size λ the perimeter is determined as follows. Starting at some arbitrary contour point (x_0, y_0), the next point on the contour (x_n, y_n), in the selected direction, usually anti-clockwise, is located in the distance d_i, $d_i = \sqrt{(x_0 - x_n)^2 + (y_0 - y_n)^2}$ as close as possible to λ. This point is then used to place the next point on the contour that satisfies the condition mentioned earlier. The process is repeated until the initial starting point (x_0, y_0) is reached. The perimeter is the sum of all distances d_i including the distance between the last

located point and the starting point. The average yardstick size is the sum of all distances d_i, excluding the distance between the last located point and the starting point, divided by the number of points found.

5. Results

The fractal image-analysis program is developed in C++ Microsoft Visual Studio. NET 2003. For analyzing brain structures in neuroanatomy changes there were used the axial T2-weighted MR data sets of different patients, which were received from Lublin hospitals. Depending on the individual subject, the number of brain slices was 22-24, and each slice is a 512×512 pixel matrix. The slices from 15 to 18±2 were analyzed from the MR data sets of each patient.

The purpose of this study was to measure the relationship between:

1) the fractal dimension of white matter and the fractal dimension of grey brain matter, the fractal dimension estimated by the box counting method being obtained:
   – (traditional method) the boxes that cover the object and the boxes which cover the border of object FD1a the fractal dimension of the white matter, FD1b – the fractal dimension of grey matter, the relationship FD1=FD1a/FD1b,
   – (modification method) the boxes that cover separately the border of the object FD2a the fractal dimension of white matter, FD2b – the fractal dimension of grey matter, the relationship FD2=FD2a/FD2b.
2) the fractal dimension, estimated by the hand and dividers method, FD3a the fractal dimension of forebrain (white matter and grey matter together) and the FD3b fractal dimension of white brain matter, the relationship FD3=FD3a/FD3b.

The same results of fractal dimension estimation are given in Table 2, where N is the number of patient.

In Table 1, where S – the slice number of MR data sets that have been analyzed, for each N given:
   – the parameters for segmentation T1 – threshold for segmentation forebrain, T2 – threshold for segmentation white brain matter;
   – the shape parameters: perimeter, area, Feret's diameter for forebrain and white brain matter, measured in pixels, pixel size = 1 x 1 mm^2

Fig. 2 presents the original images (Fig.2 a, c) numbers 1, 2 brains in neuroanatomy changes and (Fig.2 e, g) numbers 8, 12 normal brain and regions of white and grey brain matter: as can be seen in Table 2 the smaller relationship between the fractal dimensions (FD1, FD2, FD3), the more brain structures are changed (white matter decreases, grey matter increases).

Table 1. Parameters for segmentation and geometrical shape parameters

N	S	T1	T2	Forebrain			White brain matter		
				Perimeter [mm^2]	Area, [mm^2]	Feret's diameter [mm^2]	Perimeter [mm^2]	Area [mm^2]	Feret's diameter [mm^2]
1	15	55	130	1882.2	77556	342.0	4206.4	62277	331.4
2	14	51	130	1975.8	78771	350.4	5513.2	67858	341.3
3	15	38	170	1672.1	70201	323.0	3624.6	55355	313.1
4	15	49	122	1921.8	74486	333.3	4067.6	62182	328.5
5	15	49	100	1901.6	80216	356.4	3804.2	72064	344.2
6	16	42	130	1733.4	71970	328.5	3363.7	65866	323.2
7	13	41	170	1847.6	74847	332.0	3684.3	68540	330.2
8	15	40	140	1838.4	75236	338.4	3602.1	69781	335.2
9	14	50	130	1871.4	78923	343.5	3334.8	74023	343.0
10	13	42	130	1931.0	81282	356.6	3247.6	75591	345.4
11	16	42	130	1858.7	74822	329.5	3590.2	69418	326.8
12	15	36	150	1813.2	71980	327.5	3544.3	68005	324.6
13	13	48	130	3955.4	73627	349.5	3955.4	73627	349.5

N – the number of patient, S – the slice number, T1 – the threshold for segmentation forebrain

Table 2. Results of fractal dimension estimation

N	FD1a	FD1b	FD1	FD2a	FD2b	FD2	FD3a	FD3b	FD3
1	1.87961	1.67810	1.12008	1.70627	1.53890	1.10875	1.04542	1.32867	0.78681
2	1.88205	1.69560	1.10996	1.71050	1.55684	1.09870	1.05860	1.39904	0.75666
3	1.97626	1.61384	1.22456	1.79636	1.48056	1.21330	1.04486	1.32613	0.78789
4	1.91634	1.58633	1.20803	1.73806	1.46085	1.18976	1.05666	1.31054	0.80627
5	1.93219	1.50895	1.28048	1.75047	1.39630	1.25364	1.04662	1.29167	0.81029
6	1.91437	1.73492	1.26396	1.73492	1.73492	1.23464	1.04186	1.26396	0.82428
7	1.94187	1.47731	1.31446	1.75909	1.36616	1.28761	1.05090	1.27834	0.82207
8	1.95931	1.38986	1.40971	1.77397	1.30000	1.36459	1.04311	1.27088	0.82077
9	1.96138	1.41881	1.38240	1.77642	1.32610	1.33958	1.04590	1.21871	0.85820
10	1.96097	1.49328	1.31319	1.77523	1.37859	1.28770	1.04568	1.21118	0.86335
11	1.95036	1.40182	1.39130	1.76513	1.30325	1.35440	1.05228	1.27306	0.82657
12	1.94691	1.36017	1.43137	1.76363	1.27871	1.37922	1.04208	1.25008	0.83361
13	1.95829	1.46186	1.33958	1.77613	1.35950	1.30645	1.08400	1.28982	0.84042

N – the number of patient, (A)the box-counting method: 1) boxes cover the object and the border FD1a – the fractal dimension of white matter, FD1b – the fractal dimension of grey matter, FD1=FD1a/FD1b; 2) boxes cover the object FD2a – the fractal dimension of white matter, FD2b – the fractal dimension of grey matter, FD2=FD2a/FD2b, (B) the hand and dividers method: FD3a – the fractal dimension of forebrain FD3b – the fractal dimension of white brain matter, FD3=FD3a/FD3b

a) Image N=1   b)

c) Image N=2   d)

e) Image N=8   f)

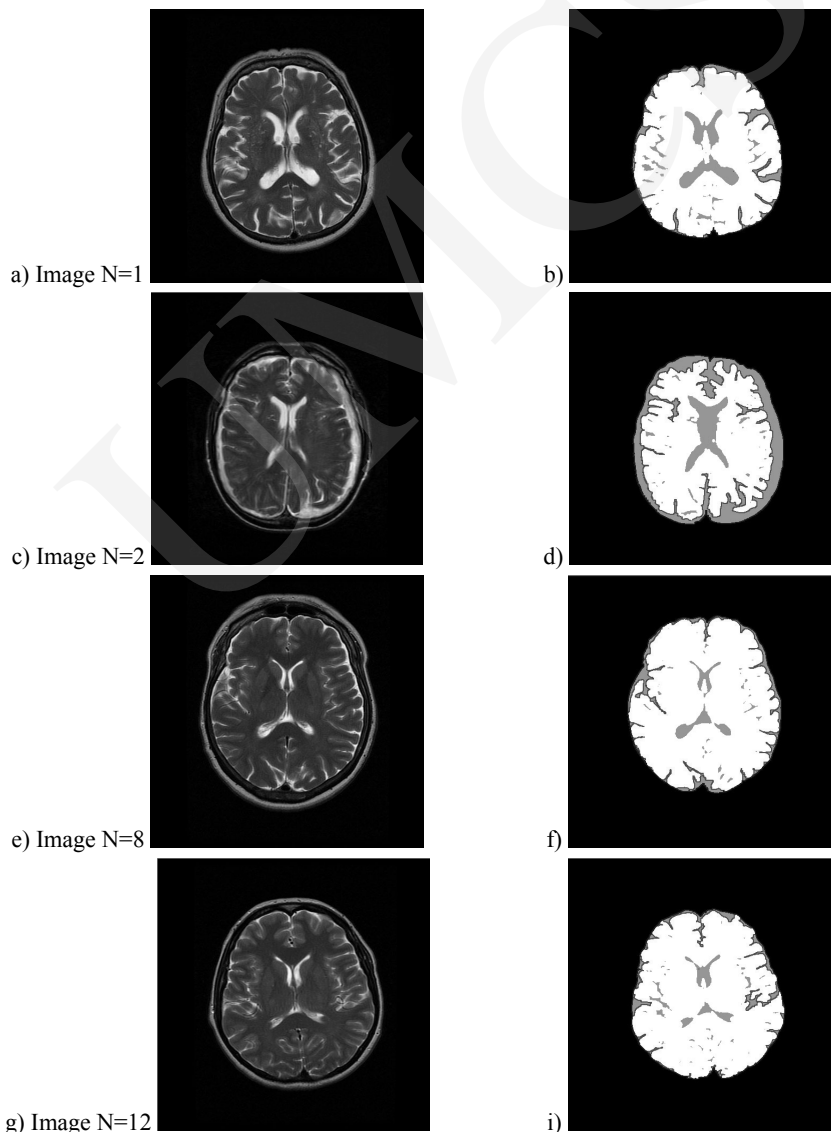g) Image N=12   i)

Fig. 2. (a, c, e, g) the original brain MR image (b, d, f, i) contours of the forebrain
and of the white brain matter

Conclusions

The objective of this study was to validate fractal analysis techniques to distinguish between the normal brain and the brain with neuroanatomy changes in dementia. We have presented a new method to examine brain structures changes in MR images: measured the relationship between the fractal dimension of white matter and the fractal dimension of grey brain matter, the fractal dimension estimated by the box counting method and the relationship between the fractal dimension of forebrain and the fractal dimension of the white brain matter, the fractal dimension estimated by the hand and dividers method.

Our results showed that the relationship between the fractal dimensions of brain with neuroanatomy changes differ from that of the normal brain. The smaller the relationship between the fractal dimensions, more brain structures changed: the white matter decreases, the grey matter increases. Our fractal analysis method could be useful for clinicians and experts in the diagnosis of neuroanatomy changes in brain structures.

References

[1] http://www.ninds.nih.gov/disorders/dementias/dementia.htm
[2] http://www.brainexplorer.org/brain_atlas/Brainatlas_index.shtml
[3] Caldwell C.B., Stapleton S.J., Hodsworth D.W., Jong R.A., Weiser W.J., Cooke G., Yaffe M.J., *Characterisation of mammographic parenchymal pattern by fractal dimension*. Physics in Medicine and Biology, 35(2) (1990) 235.
[4] Mihara N., Kuriyama K., Kido S., Kuroda C., Johkoh T., Naito H., Nakamura H.. *The usefulness of fractal geometry for the diagnosis of small peripheral lung tumors*. Nippon Igaku Hoshasen Gakkai Zasshi, 58(4) (1998) 148.
[5] Kotarski W, Widuch S., *Shape analysis of blood cells based on fractal dimension.* Journal of Medical Informatics and Technologies, 2 (2001) MI177-182.
[6] Webber R.L., Underhill T.E., Horton R.A., Dixon R.L., Pope T.L. Jr.. *Predicting osseous changes in ankle fractures.* IEEE, Engineering in Medicine and Biology Magazine, 12(1) (1993) 103.
[7] Feltrin G. P., Stramare R., Miotto D., Giacomini D., Saccavini C.. *Bone Fractal Analysis*, Current Osteoporosis Reports, 2 (2004) 53.
[8] Mandelbrot B.B., *The fractal geometry of nature*. Freeman, San Francisco, (1983).
[9] Gouyet JF, *Physics and fractal structures*, Masson, Paris, (1996).
[10] Pal. N.R., Pal S.K., *A review on image segmentation techniques*, Pattern Recognition, 26(9) (1993)1277.
[11] Zhang Y.J, *Evaluation and comparison of different segmentation algorithms*, Pattern Recognition Letters, 8 (1997) 963.
[12] Sonka M., Hlavac V., Boyle R., *Image Processing, Analysis and Machine Vision*. Chapman and Hall, (1993), (http://www.icaen.uiowa.edu/~dip/LECTURE/Segmentation1.html).
[13] Eckstein W., *Unified Gray Morphology: The Dual Rank*, Pattern Recognition and Image Analysis, 7(1) (1997) 29.
[14] Falconer K., *Fractal Geometry: Mathematical Foundations and Applications*, John Wiley & Sons Ltd., Chichester, Intercience, (1990).
[15] Kindratenko V, *Development and Application of Image Analysis Techniques for Identification and Classification of Microscopic Particles*, Universiteit Antwerpen, Ph.D. Thesis, Antwerpen, (1997), (https://netfiles.uiuc.edu/kindrtnk/www/phd/).